JOURNAL OF MATERIALS SCIENCE 9 (1974) 1536–1544

Review

Thermoplasticity, pseudoelasticity and the memory effects associated with martensitic transformations

Part 2 *The macroscopic mechanical behaviour*

R. V. KRISHNAN,* L. DELAEY, H. TAS†
Departement Metaalkunde, Katholieke Universiteit Leuven, Belgium

H. WARLIMONT
Max-Planck-Institut für Metallforschung, Stuttgart, Germany

The macroscopic mechanical behaviour (stress-strain-temperature relations in tension, compression and internal friction) associated with pseudoelasticity and the memory effects is extensively reviewed. The particular features of the tension and compression curves (the stress to induce or reorient the martensite, total elongation, reversibility and hysteresis) are analysed and their dependence on temperature and crystal orientation is discussed.

1. Introduction

In Part 1 the general characteristics of thermoelasticity, pseudoelasticity and the shape memory effects were discussed. In the present paper experimental evidence on the macroscopic mechanical behaviour is compiled to correlate the various phenomena that are associated with the martensitic transformation. Since the alloys exhibiting pseudoelasticity and shape memory effect possess a high damping capacity related to these effects, this property is also reviewed. The thermoelastic transformation either on cooling or on heating in the absence of an external stress causes no macroscopic mechanical effects. Therefore it will not be considered in the present paper.

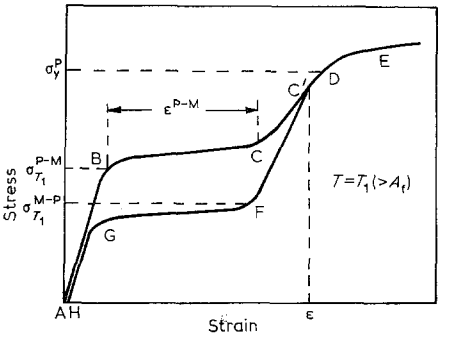

Figure 1 Schematic representation of a stress-strain curve showing the pseudoelastic behaviour. $\rho_T{}^{P-M}$ = stress necessary to cause transformation at T_1; $\rho_T{}^{M-P}$ = stress necessary for reverse transformation at T_1; $\rho_y{}^P$ = plastic yield stress of martensite at T_1; ϵ = total strain achieved; AH = irreversible component of the total strain [2].

2. Pseudoelasticity

2.1. Pseudoelasticity by martensite formation

On stressing a metastable alloy susceptible to transformation to martensite at a constant temperature, T_1, a stress-strain curve as represented in Fig. 1 is obtained, if T_1 is greater than A_f, the temperature at which the reverse transformation is completed under no stress. Section AB represents purely elastic deformation of the parent phase. At point B, corresponding to a stress level $\sigma_{T_1}{}^{P-M}$, the first martensite plates start to form. The transformation is essentially

*Present address: National Aeronautical Laboratory, Bangalore, India
†Present address: Studiecentrum voor Kernenergie (S.C.K.), Mol, Belgium

complete when point C is reached. The slope of section BC reflects the ease with which the transformation proceeds to completion. On continued stressing, the material which is in the completely transformed condition deforms elastically as represented by section CD of the curve. At D, the plastic yield point, σ_p, of the martensite is reached and the material deforms plastically until fracture occurs. If the stress is released before reaching the point D, e.g. at point C′, the strain is recovered in several stages. Part C′F of the curve corresponds to elastic unloading of the martensite. On reaching a stress ${\sigma_T}_1^{M-P}$ at F, the reverse martensitic transformation starts and the fraction of martensite decreases until the parent phase is completely restored (G). Section GH represents the elastic unloading of the parent phase. The total strain may or may not be completely recovered, the latter being the case if some irreversible deformation has taken place either during loading or during unloading. The magnitudes of ${\sigma_T}_1^{P-M}$ and ${\sigma_T}_1^{M-P}$ with respect to the yield stress, σ_y^P, of the parent at T_1 determine the actual tensile behaviour. The difference between ${\sigma_T}_1^{P-M}$ and ${\sigma_T}_1^{M-P}$ determines the stress hysteresis. The area enclosed by the loading and unloading curves gives the amount of the dissipated energy. An experimental stress-strain curve as represented in Fig. 1 was first published by Burkart and Read for indium-thallium alloys in 1953.

The stress necessary to induce the transformation, σ_T^{P-M}, has been found to be a linear function of temperature (Fig. 2). A similar relationship exists for σ_T^{M-P}. The stresses σ_T^{P-M} and σ_T^{M-P} increase with increasing temperature while the yield stress of the β phase, σ_y^P, decreases with increasing temperature, as shown in Fig. 3. The curve shown in Fig. 3 may be divided into three sections: sections AB and A′B″ correspond to stress-strain curves with a large hysteresis; sections BC and B′C′ (which differ in slope from AB and A′B″ respectively) refer to stress-strain curves with a negligible hysteresis and section CD corresponds to the deformation of the parent phase preceding the martensitic transformation.

Further variations of the stress-temperature behaviour shown schematically in Fig. 3 are due to variations of the components of applied stress in relation to the crystal orientation. In their work on In–Tl alloys Burkart and Read [1] found that the slopes of the σ_T^{M-P} and σ_T^{P-M} curves and the hysteresis vary on going from

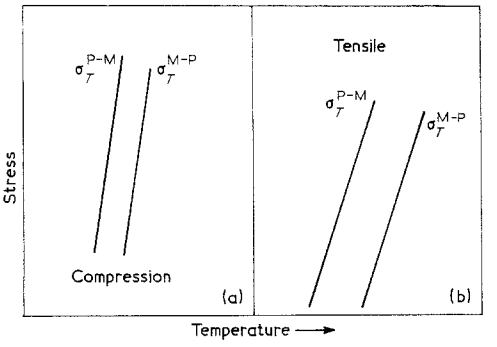

Figure 2 The effect of compressive (a) and tensile (b) loading on martensite formation and disappearance in 20.7% Tl—In alloy [1].

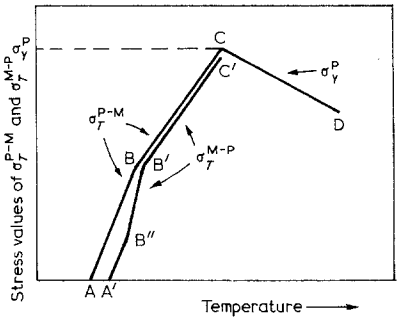

Figure 3 Variation of stress necessary to form martensite with temperature (schematic). Same symbols as in Fig. 1 [3].

tension to compression and on changing the crystal orientation.

Examples of stress-strain curves as a function of testing temperature are given in Figs. 4 and 5. Fig. 4 indicates the striking variation of σ_T^{P-M} and σ_T^{M-P} with testing temperature for Cu–Zn –Si polycrystals. Plotting these stresses against temperature, two straight lines are obtained which intersect the temperature axis ($\sigma = 0$) at M_s and A_s, respectively; these correspond to points A and A′ in Fig. 3. The further features of the σ_T^{P-M} and σ_T^{M-P} behaviour shown schematically in Fig. 3 are illustrated by the stress-strain curves of single crystals of Ag–Cd reproduced in Fig. 5. In Fig. 5a two types of curves can be differentiated regarding the stress hysteresis and the occurrence of serrations. The curves obtained at $T \geqslant 228\,K$ show nearly no serrations and a small hysteresis whilst those taken at $T \leqslant 218\,K$ show pronounced serrations and a large hysteresis. A plot of σ_T^{P-M} and σ_T^{M-P} values results in the

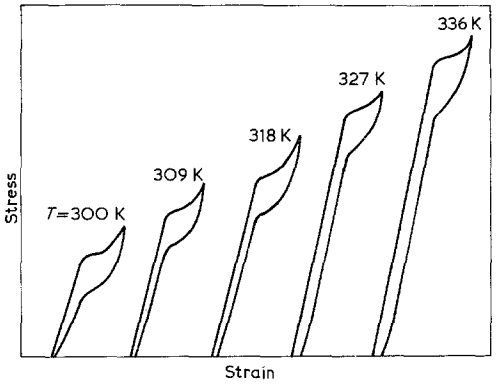

Figure 4 Stress-strain curves showing pseudoelasticity in Cu—Zn—Si alloys as a function of testing temperature [2].

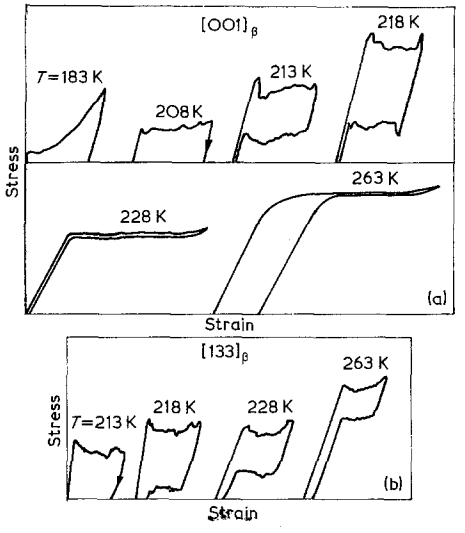

Figure 5 Stress-strain curves showing the pseudoelasticity and shape-memory effect in Ag—45 at. % Cd single crystals as a function of temperature and crystal orientation [3].

temperature dependence shown schematically in Fig. 3.

The martensite plates formed at $T < 228\,K$ grow continuously with increasing stress whereas at $T > 228\,K$ the plates grow spontaneously. In this region nucleation is stress-induced whereas growth is spontaneous, so that a stress relaxation is associated with each growth event. The absence of strain recovery on releasing the applied stress at $T \leqslant 208\,K$ indicates that no reverse transformation occurs in this temperature range. This behaviour is a prerequisite for the memory effect. The incomplete strain recovery at $T = 263\,K$ arises from plastic strain of the matrix prior to martensitic transformation whereas the reverse transformation is complete.

A comparison of Fig. 5a and b indicates that the stress-strain behaviour is a function of the orientation of the tensile axis not only quantitatively but also qualitatively.

The total transformation strain on uniaxial loading, $\epsilon_T{}^{P-M}$, varies from alloy to alloy as a function of the crystallographic parameters. The maximum strains $\epsilon_t{}^{P-M}$ reported from different measurements on single and polycrystalline specimens are given in the third column of Table I. The range of stress at which the maximum transformation strain may be obtained at different temperatures is given in the second column of Table I. The characteristic differences arising with different solvent components will be treated in Part 3. If the values of $\epsilon_t{}^{P-M}$ for single and polycrystalline specimens are compared three main points may be noted.

1. $\sigma_T{}^{P-M}$ is generally lower for polycrystalline material than for single crystal specimens. As mentioned earlier, the stress to initiate the transformation in single crystals is a function of orientation whereas in quasi-isotropic polycrystalline material the most favourable orientation is always present. Therefore the stress for the initiation of transformation in polycrystalline material should correspond to the minimum value for single crystals.

2. The maximum values of $\epsilon_t{}^{P-M}$ for single crystal specimens are given by Fig. 11a to c in Part 1, whilst the maximum strains attainable in polycrystalline specimens of the same alloy will remain lower because of the necessity of accommodation strains at grain boundaries.

3. The residual strain after releasing the stress is higher for the polycrystalline material, implying that the irreversible strain produced by one transformation cycle is higher in this case.

Although tensile or compressive stresses are emphasized as being responsible for pseudoelasticity, the macroscopic behaviour is more clearly revealed on bending. This is caused by the fact that a small linear strain gives rise to a large bending strain in thin specimens.

2.2. Pseudoelasticity by reorientation

On stressing thermal martensite, curves very similar to the ones represented in Fig. 1 are obtained, i.e. pseudoelasticity can also be obtained without being accompanied by a

TABLE I Stress necessary to induce martensite. Transformation strain of pseudoelastic martensite formation

Alloy	σ_T	ϵ_t^{P-M} (max. observed)	specimen remarks s = single crystal p = polycrystal	Strain recovery	Reference
Fe_3Be	47–66 kg mm^{-2}	± 8%	critical resolved shear stress p	± 100%–0 (after several cycles)	13
Ti—51 at. % Ni	50 × 10^{3}psi	± 1, 5%	p	100%	22
Cu—14 wt % Al—3 to 4% Ni	0–40000 psi	± 6%	from −33 to 120°C p	± 100%	4
$AuCd_{47.5}$	9 kg mm^{-2}		at 73°C S	± 100%	23
Cu–Zn–Si Cu–Zn–Sn	0–20.000 psi	15%	0 to 80°C p	± 100%	2
Cu–33%Zn–3wt%Sn	0–30.000 psi	16%	0 to 30°C s + p		17
Ag—Cd (45 at. % Cd)	0–24.000 psi	6%	−70 to 0°C s	± 100%	3

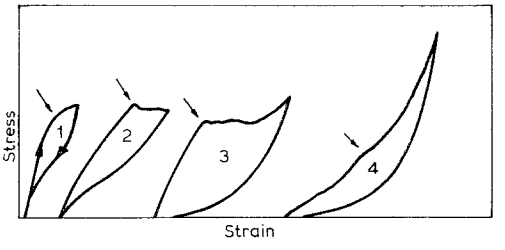

Figure 6 Stress-strain curve of Au—Cd alloys showing pseudoelastic behaviour as a function of the number of cycles [9].

martensitic phase change. This pseudoelasticity is obtained by reorientation. It has been observed in Au–Cd [5], In–Tl [6], Cu–Al–Ni [7], Cu–Al [8] alloys. The stress necessary to initiate the reorientation decreases with increasing number of transformation cycles. This behaviour is shown for an Au–Cd alloy in Fig. 6 [9]. Since the reorientation of the martensite plates can be envisaged as a form of twinning in most cases ([10, 11], see also Part 1), the pseudoelasticity obtained by reorientation can be compared to elastic twinning and untwinning in crystals. Elastic twinning refers to the process of deformation in which a twin, which appears in the crystal upon the application of an external stress, changes its dimensions reversibly with any change in the magnitude of the applied stress. Elastic twinning has been treated extensively by Kosevich and Boiko [12] and by Bolling and Richman [13]. A hysteresis is also observed for elastic twinning; it is considered to arise from a resistive energy similar to that arising from dry friction and from an interfacial energy. Sumino [14] included Au–Cd and In–Tl martensites in his study of the mechanical behaviour of crystals with twinned microstructure. He concluded that the experimental data on these alloys (as in Fig. 6) could not be interpreted in terms of conventional theory of twinning. In fact, the problem is not to consider the nucleation of a twin but rather the motion of existing twin boundaries.

In considering the growth of deformation twins at low stresses, the structural defects of existing twin boundaries have to be taken into account; more specifically, ledges along twin boundaries are highly mobile. Consequently, the stress necessary for twinning along a twin boundary is considerably lower than for twin formation in a bulk crystal. The ratio of the two theoretical shear stresses could be as low as 1/100 in the case of Au–Cd alloy.

The deformation of a martensitic structure capable of reorientation requires a finite applied stress. The process consists essentially of converting martensite of a given variant into a variant of more favourable orientation. It is to be expected that mobile defects exist along the martensite plate boundaries such that an applied stress will give rise to their motion, yielding maximum elongation in the direction of that stress. It has been suggested that the progressing interface sweeps out the existing defects [14]. This possible mechanism along with the activa-

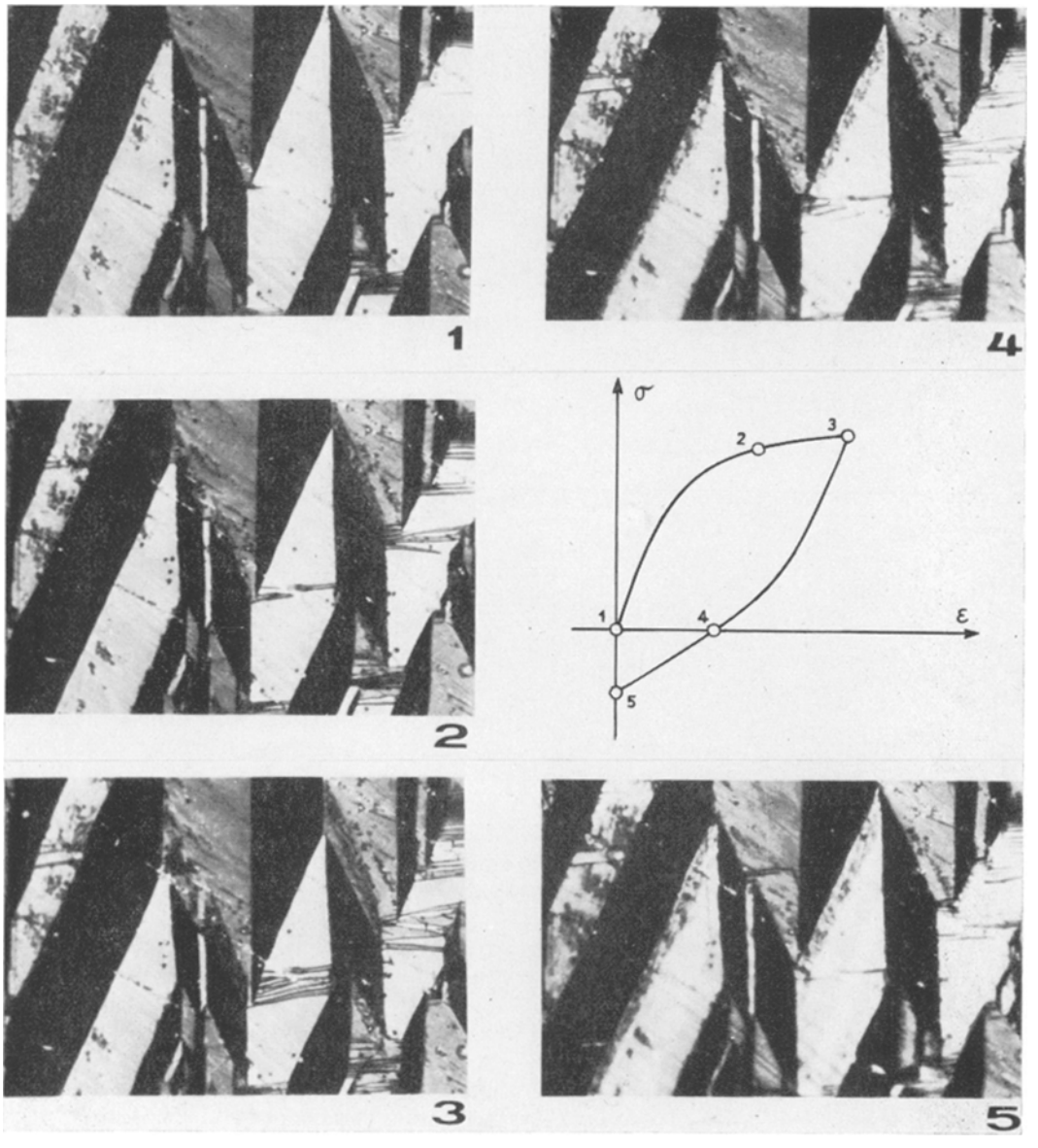

Figure 7 Stress-strain curve and the associated micro-structures of a Cu—Zn—Al—Ni 3R-type of martensite, showing partial pseudoelastic behaviour (1 to 4). 4 and 5 represents the shape recovery (shape memory effect) of the residual strain while heating.

tion of suitably oriented mobile defects in the interfaces during the first loading cycle can explain the decrease in the stress for the onset of reorientation in subsequent cycles.

Other mechanisms for the reorientation of the martensite plates have been proposed by Wasilewski [26]. He concludes that while a suitable stress is applied above M_S the forward austenite-to-martensite transformation can always occur, but that while a stress is applied below A_S only some combinations of stress-and-variant-orientation can lower the start temperature for the reverse transformation, martensite-to-austenite. Therefore the temperature A_d is the equivalent of M_d as determined for a specific transformation variant and not for the onset of the transformation regardless of the variants formed. In his review on the nature of martensitic

transformations, Wasilewski concludes further that, if the martensite is stressed between M_f and A_d, ($A_d < M_f$), the stress-assisted austenite reversion is only a transient intermediate step, which is followed by the immediate and also stress-assisted transformation of this austenite to another martensite variant of orientation different from that of the original martensite.

The experimental differentiation between the pure motion of a martensite plate boundary and the model proposed by Wasilewski will be very difficult. In Fig. 7, five micrographs out of a series are reproduced, showing the to-and-fro movement of such a martensite plate boundary on stressing (1 to 3), the forward movement on releasing (3 to 4) and heating (4 to 5) the sample. As is shown in a film published in *Encyclopedia Cinematographica* [25], Wasilewski's two-step mechanism cannot be made visible, but there are indications [27] that this two-step mechanism can occur on an atomic scale. In crystallographic terms the two models are therefore equivalent, only the atomic position before and after the application of the stress is considered but not the path followed by the atoms.

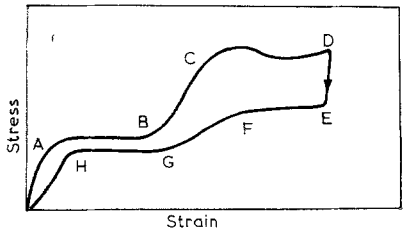

Figure 8 Stress-strain curve for a single crystal of Cu—Al—Ni alloys at 38° C, with a pseudoelastic strain up to 24% [7].

2.3. Pseudoelasticity by the combined formation and reorientation of martensite

A multistage stress-strain curve of the type shown in Fig. 1 need not be caused by transformation followed by plastic deformation; it may also be due to transformation followed by reorientation. A curve reported by Busch *et al.* [7] shown in Fig. 8 may be interpreted on this basis. Martensite formation sets in at point A and continues until point B is reached. In section BC the martensite is stressed elastically whereas we surmise that reorientation takes place in section CD. Upon unloading, both stages of the process are reversed. This example shows that pseudoelasticity occurs not only on stressing thermal martensite but also on stressing stress-induced martensite. It appears that in this case the stress level for the formation of stress-induced martensite is less than that required for its reorientation.

2.4. Internal friction and fatigue

Several of the alloys listed in Table I of Part 1, show a very high damping capacity. They also possess favourable fatigue properties. Simple experiments like bouncing a ball [15] or striking a strip of material susceptible to pseudoelastic behaviour at different temperatures can demonstrate that the damping behaviour is a sensitive function of temperature. This is associated with the temperature dependence of the amount of martensite formed.

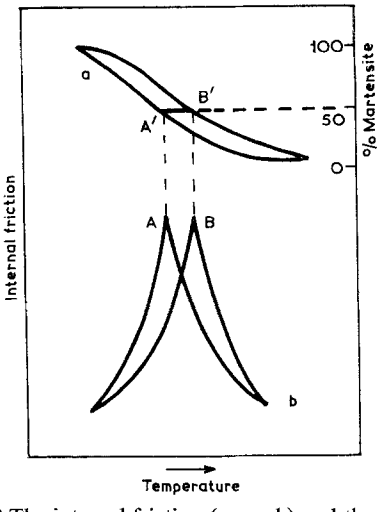

Figure 9 The internal friction (curve b) and the electrical resistivity (curve a) in the temperature range of the formation of thermoelastic martensite in a Cu—Al—Ni alloy [16].

The relation between internal friction and the amount of martensite at a given temperature in a Cu—Al—Ni alloy is shown in Fig. 9 [16]. Curve a shows the amount of martensite present during heating and cooling whilst curve b gives the corresponding changes in internal friction as a function of temperature. The maxima (A and B) in internal friction occur at temperatures corresponding to 50% martensite present in the specimen (points A′ and B′).

The mechanism giving rise to internal friction in pseudoelastic alloys has not been fully established. It is related to the energy dissipation which is part of the resistive energy reflected by the hysteresis in the stress-strain curves. The elementary mechanism of internal friction is associated with the movement of the interphase, interplate and/or twin boundaries. In Mn—Cu alloys the internal friction was found to exhibit a main peak, associated with the movement of twin boundaries, and a sub-peak associated with the movement of the interphase fcc–fct [28].

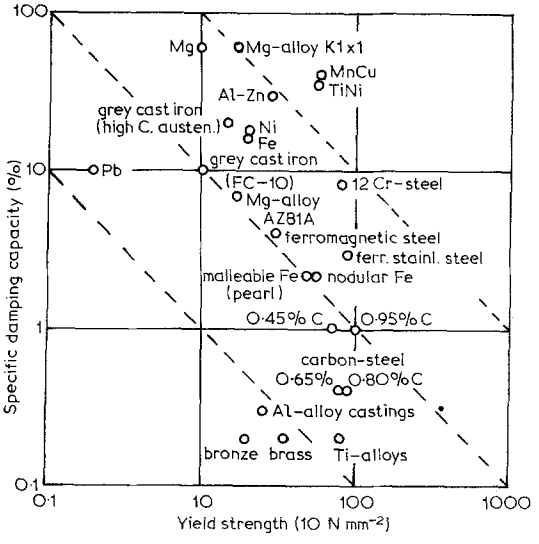

Figure 10 Specific damping capacity as a function of the yield stress for various materials [24].

The specific damping capacity in combination with the yield strength is the joint criterion for technological application of highly damping materials. Fig. 10 shows a plot of these two properties for a number of materials. It is evident that some of the pseudoelastic alloys show a favourable combination of both.

Another particular property of pseudoelastic alloys is their high fatigue strength. An Ni—Ti alloy has been shown to sustain 10^7 cycles before fracture at a stress level of 70×10^3 psi [15]; a Cu—Al—Ni alloy exhibited a fatigue life 10^2 times that of brass at 2% total strain [7]. Preliminary microstructural investigations indicate that this behaviour is based upon the relaxation of stress concentrations by pseudoelastic martensite formation.

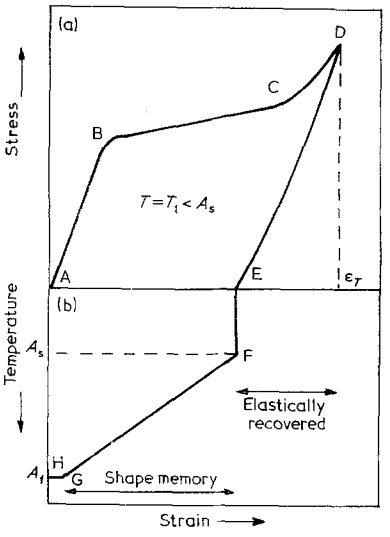

Figure 11 Schematic representation of a stress-strain curve showing the shape-memory effect by martensite formation or reorientation: (a) the deformation stage; (b) the shape recovery while heating the specimen.

3. Memory effect by transformation and reorientation

In contrast to pseudoelasticity, the shape memory effect is achieved by deforming the material at one temperature and heating it up to a higher temperature. It recovers its original shape during heating. Fig. 11, which is a more detailed drawing equivalent to Fig. 1c of Part 1, illustrates the process schematically. The rising portion of the curve (up to point D in Fig. 11) is due either to the formation of stress-induced martensite or to the reorientation of the existing thermally induced martensite. On unloading at this temperature, the material recovers elastically first. The recovery of the remaining strain is due to either transformation or reorientation. In the ideal case, strain recovery is complete (the whole of AE in Fig. 11). If the material is heated recovery commences at a temperature A_s (at F) and continues until G, corresponding to temperature A_f, is reached. Strain recovery is never complete because along with the stress-induced transformation some plastic strain will occur which is not recovered on heating to A_f. Thus the total strain of the material consists of (a) the elastically recoverable strain, (b) the reversible strain accompanying the transformation and/or reorientation, and (c) the irreversible plastic strain (GH).

For stress-induced martensite, the stress at

point B is a function of temperature given by the thermodynamic functions associated with the transformation (see Part 3) and it corresponds to σ_T^{P-M} in Fig. 1. In the case of reorientation, the stress at B is determined by the stress required for the displacement of plate and twin boundaries; its temperature dependence is given by that of the elastic constants of the martensite. The temperature at which the strain recovery commences will be close to $A_S \lesssim A_S^0$ where A_S^0 is the temperature corresponding to the onset of reverse transformation after thermal martensite formation.

The strain recovery is not always associated with one unique process. For example, a deformed In–Tl specimen recovers in two distinct stages [8]. The first stage occurs below A_S^0. It is due to the partial reverse movement of the twin boundaries, i.e. reorientation, which in this case, is aided by the temperature dependence of the tetragonality of the martensite. At A_S the remaining strain is recovered drastically as the specimen transforms back to the fcc parent phase.

Pseudoelasticity and the shape memory effect are very closely related. As shown in Fig. 5a and b, the amount of strain recovered during the unloading cycle is a function of testing temperature. The strain that is not recovered isothermally is recovered during heating. In other words, strain recovery by the pseudoelastic mechanism and by the shape memory mechanism are complementary. This relation has been established for Ag–Cd [3] and Cu–Zn–Sn single crystal specimens [17] and is shown for the latter in Fig. 12.

Since martensitic transformation and reorientation are the basis of the memory effect, any other transformation that precedes the martensitic transformation and reduces the volume fraction of parent phase will reduce the absolute magnitude of recoverable strain.

4. Transformations under constant load or constant strain

In a number of investigations where martensitic transformations were induced by temperature changes under constant load, the effects discussed in this paper were also observed. Most of the experiments were carried out on Fe–Ni [18-20] and Cu–Zn [24]. The fractions of recoverable transformation strain and irreversible plastic strain are sensitive functions of the applied stress. An example of complete strain recovery which

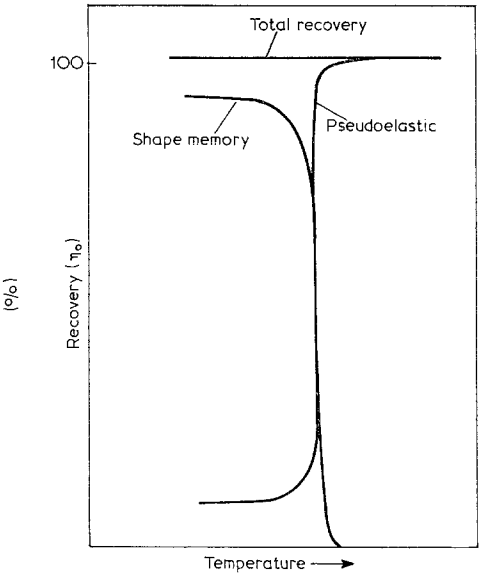

Figure 12 The total shape recovery and the shape recovery by pseudoelasticity and shape memory effect (Cu—Zn—Sn single crystal) [17].

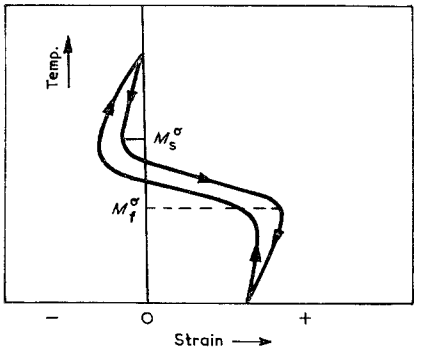

Figure 13 The shape deformation obtained by cooling and heating a Cu—Zn crystal under load [21].

occurred at comparatively low stress is shown in Fig. 13 [21].

On cooling the specimen initially shrinks owing to thermal contraction. On reaching M_S^σ, which is a function of the applied stress, the specimen begins to transform and this continues until M_f^σ is reached, where the transformation is complete.

When the external stress is increased below the yield stress of the parent phase, the transformation strain is increased. In addition to the reversible fraction an irreversible fraction is also obtained. This irreversible component was

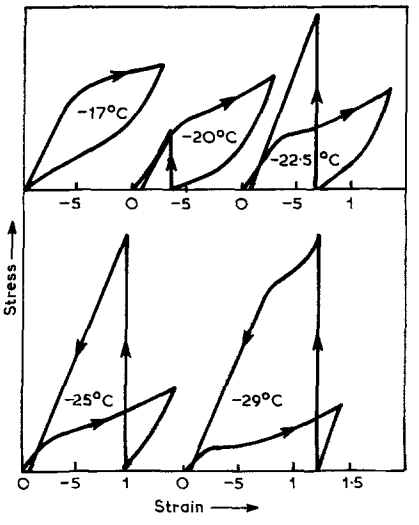

Figure 14 Stress-strain curves of Cu—Zn—Sn alloys showing the pseudoelastic behaviour and the shape memory effect as a function of temperature. The samples with a residual strain after releasing the stress have been heated under constant strain. Stresses are built up and are released by releasing the strain [17]. The first set of curves showing the pseudoelasticity and memory effect can be compared with Figs. 1 and 11. The second set of curves indicates how the stress increases while heating the sample in the strained state (vertical line). Upon releasing the strain the stress automatically drops.

termed *transformation plasticity* (Umwandlungsplastizität). If the applied stress exceeds the yield point, the irreversible component increases still further. It is assumed that the yield point is lowered during the transformation and that no increase in stress is required to maintain flow. The large elongation is attributed to crystallographic slip occurring during the transformation.

If after stress-induced transformation the strain is kept constant while the temperature is increased, a considerable increase in stress results. This is due to the driving energy of the reverse transformation which is exerted as a stress since the transformation is restrained. This behaviour is illustrated in Fig. 14 for a Cu–Zn –Sn alloy [17].

References

1. M. W. BURKART and T. A. READ, *Trans. Met. Soc. AIME* **197** (1953) 1516.
2. H. POPS, *Met. Trans.* **1** (1970) 251.
3. R. V. KRISHNAN and L. C. BROWN, *ibid* **4** (1973) 423.
4. K. OISHI and L. C. BROWN, *ibid* **2** (1971) 1971.
5. H. K. BIRNBAUM and T. A. READ, *Trans. Met. Soc. AIME* **218** (1960) 662.
6. Z. S. BASINSKI and J. W. CHRISTIAN, *Acta Met.* **2** (1954) 148.
7. R. E. BUSCH, R. T. LUEDEMAN and P. M. CROSS, U.S. Army Material Research Report, AD 629726 (1966).
8. A. NAGASAWA, *Phys. Stat. Sol.* (*a*) **8** (1971) 531.
9. T. AOYAGI and K. SUMINO, *ibid* **33** (1969) 317.
10. C. M. WAYMAN and K. SHIMIZU, *Met. Sci. J.* **6** (1972) 175.
11. H. TAS, L. DELAEY and A. DERUYTTÈRE, *Z. Metallk.* **64** (1973) 855, 862.
12. A. M. KOSEVICH and V. S. BOLKO, *Sov. Phys. Uspekhi* **14** (1971) 286.
13. G. F. BOLLING and R. H. RICHMAN, *Acta Met.* **13** (1965) 709.
14. K. SUMINO, *Phys. Stat. Sol.* **33** (1969) 327.
15. W. J. BUEHLER and F. E. WANG, *Ocean Eng.* **1** (1968) 105.
16. I. A. ARBUZOVA, V. S. GAVRILYUK and L. G. KHANDROS, *Fis. Metal. Metalloved.* **27** (1969) 1126.
17. J. D. EISENWASSER and L. C. BROWN, *Met. Trans.* **3** (1972) 1359.
18. G. WASSERMANN, *Arch. Eisenhüttenw.* **6** (1932/33) 347; **10** (1936/37) 321; and **11** (1937/38) 89.
19. E. SCHEIL and W. THIEHL, *ibid* **10** (1936/37) 477.
20. H. P. SATTLER and G. WASSERMANN, *J. Less-Common Metals* **28** (1972) 119.
21. E. HORNBOGEN and G. WASSERMANN, *Z. Metallk.* **47** (1956) 427.
22. R. J. WASILEWSKI, *Scripta Met.* **5** (1971) 127.
23. N. NAKANISHI, Y. MURAKAMI and S. KACHI, *Phys. Letters* **37A** (1971) 61.
24. M. SUGIMOTO, private communication.
25. L. DELAEY and G. HUMMEL, Film: Institut für den Wissenschaftlichen Film Göttingen. *Encyclopedia Cinematographica* (1974).
26. R. J. WASILEWSKI, *Met. Trans.* 2 (1971) 2973 and *Scripta Met.* 5 (1971) 207.
27. H. TAS and L. DELAEY, to be published.
28. K. SUGIMOTO, T. MORI, and S. SHIODE, *Met. Sci.* 7 (1973) 103.

Received 1 February and accepted 19 February 1974.